RC22715 (W0302-009) February 3, 2003
Materials Science

IBM Research Report

Study of IMC Morphologies and Phase Characteristics Affected by the Reactions of Ni and Cu Metallurgies with Pb-Free Solder Joints

Won Kyoung Choi, Sung K. Kang*, Yoon Chul Sohn, Da-Yuan Shih***

Samsung Advanced Institute of Technology,
P.O. Box 111, Suwon, 440-600, Korea

*IBM T.J.Watson Research Center,
1101 Kitchawan Rd., Rt. 134,
Yorktown Heights, NY 10598

**Dep. of Mater. Eng., KAIST, 373-1,
GuSeong-Dong, Yuseong-Gu,
Daejeon, Korea

Research Division
Almaden - Austin - Beijing - Delhi - Haifa - India - T. J. Watson - Tokyo - Zurich

Study of IMC Morphologies and Phase Characteristics Affected by the Reactions of Ni and Cu Metallurgies with Pb-Free Solder Joints

Won Kyoung Choi, Sung K. Kang*, Yoon Chul Sohn** and Da-Yuan Shih*
Samsung Advanced Institute of Technology, P.O. Box 111, Suwon, 440-600, Korea
*IBM T.J.Watson Research Center, 1101 Kitchawan Rd., Rt. 134, Yorktown Heights, NY 10598
**Dep. of Mater. Eng., KAIST, 373-1, GuSeong-Dong, Yuseong-Gu, Daejeon, Korea

ABSTRACT

Most Pb-free solders proposed to replace Pb-containing solders for microelectronic applications are Sn-rich solders with a higher melting point than the eutectic Sn-Pb solder. Due to their higher Sn content and higher reflow temperatures, the interfacial reactions between Sn-rich solders and the commonly used pad metallurgies such as Cu or Ni are found to be more aggressive and, therefore, become a concern that may affect the integrity and reliability of the solder joint. The interfacial microstructures on Ni layer have been investigated in terms of intermetallic compound (IMC) morphology and its growth kinetics. Cu, when plated either as an underlayer or overlayer on Ni, is shown to influence the interfacial reactions, which is also affected by the characteristics of Ni plating and reflow conditions. As a result, an in-depth study has been carried out to understand the interfacial reactions between Pb-free solder and Ni (both electro- and electroless plated) by comparing the IMC morphology and phase identification. The three variables that have been investigated in this study include types of Ni plating, Ni thickness, and reflow conditions. The effects of Cu under- and over-layer on Ni are also examined by varying both Cu and Ni thickness. Based on this study, it was found that the type of Ni plating affects the IMC morphology significantly. A compact structure of Ni-Sn IMC was identified on electrolytic Ni, and a porous structure on electroless Ni. In addition, Ni thickness as well as reflow time also affect the IMC phases formed at the interface with the presence of a Cu layer. When a thin Cu layer is plated over Ni and subsequently reacted with Sn solder, the interfacial microstructure and IMC phases strongly depend on the Cu thickness. For thin Cu layer, Ni-Sn IMC is the dominant phase, while Cu-Sn IMC is the major phase for thick Cu. The results obtained in this study have provided a more detailed understanding of the interfacial reactions, which leads to the designing of a more reliable metallurgical system for Pb-free solder joints.

INTRODUCTION

Flip-chip solder interconnect structure generally consists of the solder bump, an under bump metallization (UBM) layer which are built on top of a wafer [1]. Recently, the electronic industry has made significant effort in the development and qualification of an optimal Pb-free solder alloy for flip-chip solder bumps. The Pb-free solder candidates include Sn-3.5wt%Ag (m.p. 221^{o}C), Sn-0.7wt%Cu (m.p. 227^{o}C), Sn-3.8wt%Ag-0.7wt%Cu (m.p. 217 ^{o}C), Sn-5wt%Sb (232-240^{o}C) among others. Since all these alloys have high Sn content, they react more heavily with the UBM than the conventional Pb-rich solder bumps. Hence, to search for a UBM structure more stable against Pb-free solder reactions has been a subject of many investigations. Another issue associated with the fabrication of Pb-free solder bumps is to precisely control the alloy composition.

In order to control the severe reaction between the molten Sn and UBM, a Ni layer has been introduced as a reaction barrier in the UBM structure, since Ni reacts with the molten Sn at a slower rate than Cu. For comparison purpose, both electrolytically plated Ni and electrolessly plated Ni-P have been included in the study.. The reaction between Pb-free solders and Ni has been investigated in terms of intermetallic compound (IMC) morphology and growth kinetics. The different types of Ni plating, electrolytic or electroless, have been reported to produce different interfacial reaction products in Pb-free solder joints [2,3]. The morphologies of Ni-Sn IMC appear different between electrolytic- plated Ni and electroless- plated Ni-P [2]. The dissolution of electrolytic-plated Ni into Pb-free solder was reported to be slower than the electroless-plated Ni-P during reflow [3]. In this study, a systematic investigation is performed to evaluate the difference in Ni platings in the reaction with molten Sn.

It was also reported that with the addition of even a small amount of Cu in Sn-based solders the reactions with Ni are affected, due possibly to the preferential reaction between Sn and Cu [4-8]. By increasing the Cu content, the IMC phases change from $(Ni,Cu)_3Sn_4$ type to $(Cu,Ni)_6Sn_5$ and this transition happens at around 0.5 wt % Cu [7,8]. These findings suggest that the Cu under- or over-layer on Ni UBM may also influence the interfacial reactions between a Sn-rich solder and Ni. When Cu exists under the Ni layer, under a thin Ni layer, Cu could react with the molten solder by out-diffusion through the Ni layer, or directly in contact with the molten solder when the Ni layer is totally consumed. When Cu is placed on top of the Ni layer, the reaction product may vary according to the Cu thickness.

In this study the presence of a Cu layer either under or over the Ni layer has been evaluated by varying the thickness of Cu and Ni. The type of Ni plating, either electrolytic or electroless, serving as a reaction/diffusion barrier, has also been investigated in the study.

EXPERIMENTAL PROCEDURE

Sample Preparation

Cu foils (25μm in thick) were used as a substrate. Its surface was cleaned in acetone and treated in a 0.5M H_2SO_4 solution to remove surface oxides. Both electrolytic Ni and electroless Ni-P were plated on a Cu foil of a different thickness such as 0.3, 0.6, 1, 3 and 10 μm. The electrolytic Ni plating was performed on a cleaned Cu foil in a nickel sulfamate solution (3.6 pH) with 3.75 A/dm^2 at 50 ^{o}C. For the electroless Ni-P, a Cu foil was activated with a Pd solution before the plating. A Ni-P layer was electrolessly deposited on the Pd-activated Cu foil in a Ni plating solution (Technic EN9185) at 90 ^{o}C (4.9 pH). The P content in the Ni-P layer was measured to be 16 at% (9 wt%) by an electron microprobe analyzer (EMPA). As a Pb-free solder, 40 μm Sn was electroplated on Ni-coated Cu foils using a Lea Ronal Sn plating solution (Shipley Co.) at a current density of 50 mA/cm^2. The Sn thickness of 40 μm was chosen in order to reproduce the solder volume comparable to flip-chip solder bumps in use. The Cu plating was done in a Cu sulfate bath at a current density of 37.5 mA/cm^2. The Cu thickness was chosen from 0.04 to 0.5 μm, to produce the Sn-Cu alloy compositions between 0.1 and 1.4 wt% Cu under the assumption that the entire Cu would melt in the liquid Sn of 40 μm during reflow.

These samples were subjected to the reflow for 2 and 10 min. at 250 ^{o}C on a hot plate covered by an aluminum lid so as to maintain the temperature constant and to purge N_2 gas in it. Here, the reflow time was measured as the total time for a sample sitting on the hot plate, including the heating time. Thus, the real reflow time for the temperature above 232^{o}C (Sn melting temp.) may be slightly shorter than 2 or 10 min.

Characterization

The cross-section and top views of IMC morphologies were observed with scanning electron microscopy (SEM) operated at 25 kV. The IMC composition was analyzed with energy dispersive spectroscopy (EDS). To identify the crystal structure of IMCs formed at the interface, X-ray diffraction (XRD) analysis (λ_{Cu}=1.5418 μm) was performed after removing the unreacted Sn. The Sn was etched off in the mixed solution of $HCl:HNO_3:CH_3OH$ for several hours at room temperature. To prepare the cross-sectional samples, the reflowed samples were mounted in room temperature to cure epoxy, cross-sectioned using a diamond saw, and then prepared metallographically to a final finish of 0.05 μm alumina slurry. The surface of cross-sectioned samples was etched with $HCl:HNO_3:CH_3OH$ solution for several minutes to enhance the contrast in SEM. A thin layer of Au was also coated on each cross-sectioned sample for SEM observation.

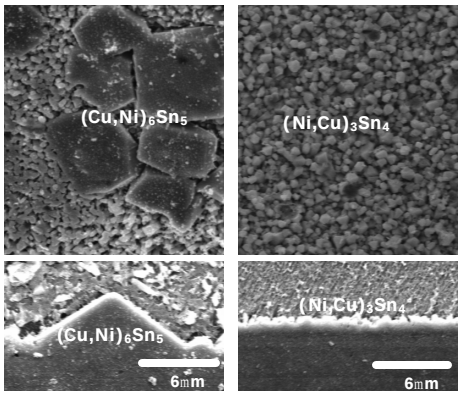

Fig.1. SEM micrographs of IMC morphologies o Cu/Ni(ED)/Sn samples in the top and the cross-sectional views after reflow for 2 min at 250ºC; on (a) 0.3 ㎛ Ni (ED) and (b) 0.6 ㎛ Ni (ED)

RESULTS

IMC Morphologies and Phases in Cu/Ni(ED)/Sn

Fig. 1 exhibits SEM micrographs of IMC morphologies in the cross-section and the top views on 0.3 and 0.6 μm Ni(ED), which were reflowed for 2 min at 250^{o}C. In all the samples except for 0.3 μm Ni(ED), Ni_3Sn_4 is found as a major layer at the interface. The 0.3 μm Ni layer seems to dissolve completely into the molten Sn to form chunky $(Cu,Ni)_6Sn_5$ grains, occupying the interface mostly as shown in Fig. 1(a). The cross-sectional view of $(Cu,Ni)_6Sn_5$ shows a pyramid shape, similar to the morphology reported by Chen et al. [7]. The ternary $(Cu,Ni)_6Sn_5$ has found to have the same crystal structure as the binary Cu_6Sn_5 phase [6-8] and about the half amount of Cu sites in the Cu_6Sn_5 phase was replaced with Ni [3-8]. Ni_3Sn_4 grains shown on 0.6 μm Ni have a faceted and angular morphology and constitute a compact layer as noted in Fig. 1(b). For 2 min reflow, the 0.6 μm Ni did not dissolve completely and formed some $(Ni,Cu)_3Sn_4$. The presence of Cu atoms in $(Ni,Cu)_3Sn_4$ was confirmed by an EDS analysis. This suggests some Cu atoms from the underlayer participated to form the ternary Ni-Cu-Sn

intermetallics.

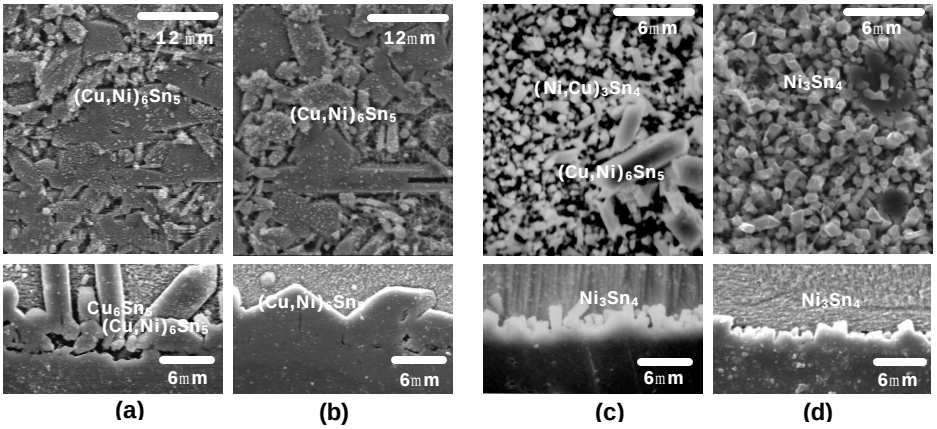

Fig. 2. SEM micrographs of IMC morphologies of Cu/Ni(ED)/Sn samples in the top and cross-sectional views after the extended reflow for 10 min at 250°C: on (a) 0.3 mm Ni(ED), (b) 0.6 mm Ni(ED), (c) 1 mm Ni(ED) and (d) 3 mm Ni(ED)

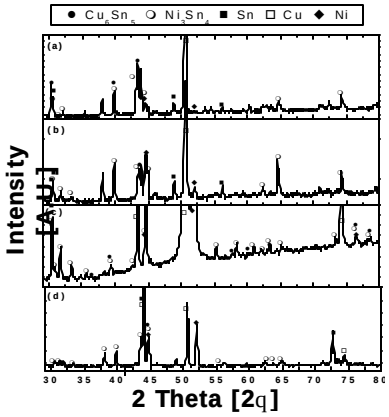

Fig.3. XRD patterns obtained from Cu/Ni(ED)/Sn samples ; (a) 0.3 and (b) 0.6 mm Ni(ED) layers after 2 min reflow and (c) 1 and (d) 3 mm Ni(ED) layers after 10 min reflow.

Fig. 2 shows SEM micrographs of IMC morphologies in the top and cross-sectional views after an extended reflow, 10 min at 250°C. For 0.3 μm Ni and 0.6 μm Ni, chunky $(Cu,Ni)_6Sn_5$ IMCs have grown aggressively all over the interface as shown in the top views of Fig.2(a) and 2(b). In addition, rod-like η-Cu_6Sn_5 grains without containing Ni are seen in the cross-section of 0.3 μm Ni. These Cu-Sn IMCs appear to be detached from the interface, suggesting the thin Ni layer dissolved completely during the reflow. For 1 μm Ni, the $(Ni,Cu)_3Sn_4$ IMC is observed as the dominant phase, while the chunky $(Cu,Ni)_6Sn_5$ IMC is noted occasionally in Fig. 2(b). For 3 μm and 10 μm Ni, only the angular Ni_3Sn_4 are detected as in Fig. 2(c) and (d), indicating the Cu underlayer was not involved in the interfacial reactions even for 10 min reflow. By comparing between Cu-Sn and Ni-Sn type IMCs, it is confirmed the Cu-Sn type IMC grows much faster than the Ni-Sn type under the conditions investigated.

XRD analysis has been employed to identify the IMC phases formed at the interface for all samples. It is noted that the Ni_3Sn_4 phase is the first forming IMC on Ni layer, because the Ni_3Sn_4 peaks are detected in all samples, although the peaks are very small on 0.3 μm Ni. Fig. 3 represents the XRD patterns obtained from the samples of different Ni thickness and reflow time. For 0.3 μm Ni with 2 min reflow, Fig. 3(a), the η-Cu_6Sn_5 peaks are stronger than the Ni_3Sn_4. But, the η-Cu_6Sn_5 peaks are not seen for 0.6 μm Ni after 2 min in Fig. 3(b). After 10min reflow, Ni_3Sn_4 peaks are noted with the small peaks of η-Cu_6Sn_5 on 1 μm Ni, as shown in Fig. 3(c). However, for 3 μm Ni, only Ni_3Sn_4 peaks are found even after 10 min reflow, in Fig. 3(d).

IMC Morphologies and Phases in Cu/Ni-P(EL)/Sn

The interfacial reactions on electroless Ni-P samples are examined in comparison with those on electrolytic Ni. Fig. 4 shows the IMC morphologies in the top and cross-sectional views after reflow at 250°C for 2 min. The IMC morphologies on Ni-P(EL) look quite different from those on Ni(ED). For 0.6 μm Ni-P(EL), the $(Ni,Cu)_3Sn_4$ phase is shown as fine, needle-like shape, generating a porous structure, in Fig.4(b), while for 0.3 μm Ni-P(EL), three types of

IMCs, $(Cu,Ni)_6Sn_5$, η-Cu_6Sn_5 and $(Ni,Cu)_3Sn_4$ are found, in Fig. 4(a). From the top-view, a colony-type $(Cu,Ni)_6Sn_5$ of tiny grains is revealed.

For the long reflow time of 10 min, the IMCs have grown further. The $(Ni,Cu)_3Sn_4$ on the electroless Ni-P seems to grow even faster than on the electrolytic Ni(ED). The η-Cu_6Sn_5 on 0.3 μm and 0.6 μm Ni forms a continuous layer close to the Cu underlayer as indicated in Fig. 5(a) and (b). For 0.3 μm Ni, the rod-like η-Cu_6Sn_5 IMC was separated from the interface, but no Ni_3Sn_4 was observed at all. For thick Ni of 3 and 10 μm, the needle-like $(Ni,Cu)_3Sn_4$ has grown in random directions, resulting in a porous structure of a thicker IMC.

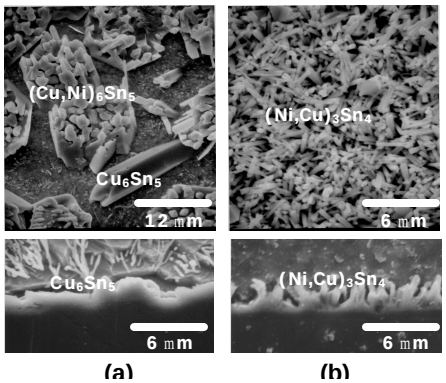

Fig.4. SEM micrographs of IMC morphologies of Cu/Ni(EL)/Sn samples in the top and cross-sectional views after reflow for 2 min at 250°C; on (a) 0.3 mm Ni-P (EL) and (b) 0.6 mm Ni-P (EL)

Fig. 6 presents the XRD patterns from the electroless Ni-P samples reflowed at 250 °C for 2 and 10 min. For 0.3 μm Ni with 2 min reflow, both Ni_3Sn_4 and Cu_6Sn_5 were observed in Fig. 6(a), but only Ni_3Sn_4 was observed for 0.6 μm Ni in Fig. 6(b). However, after 10 min reflow on 0.3 μm Ni, only the η-Cu_6Sn_5 phase was identified, not Ni_3Sn_4 phase in Fig. 6(c). For thick, electroless Ni-P, 3 μm and 10 μm, Ni_3Sn_4 phase was detected alone. In Fig. 6(d), it is noted that the 10 μm Ni-P (EL) is still in an amorphous state by judging from the broad Ni peak around 45°. In addition, small peaks from the Ni_3P phase were found, as well.

<u>Interfacial Microstructures and Phases in Cu/Ni(ED)/Cu(ED)/Sn</u>

The interfaces having an electrolytic Cu between Ni(ED) and Sn(ED) layers were investigated. In this case, it is expected that the Cu thickness would affect the interfacial reaction significantly depending upon the Ni(ED) thickness and reflow time. Fig. 7 shows the IMC morphologies on Ni(1 μm)i/Cu (0.04 μm) and Ni(3 μm)i/Cu(0.1 μm) in the top and cross-sectional views after 2 and 10 min reflows, respectively. For both cases, the Cu was thin enough to be dissolved into the molten Sn entirely during the reflow. Thus, $(Ni,Cu)_3Sn_4$ is present at the interface after 2 min in both samples, in Fig. 7(a) and (c). As the reflow time increases to 10 min, some $(Cu,Ni)_6Sn_5$ grains were formed in addition to the major phase, $(Ni,Cu)_3Sn_4$, on Ni(1μm)/Cu(0.04μm), in Fig. 7(b). It indicates that the Cu atoms from the underlayer contributed to the interfacial reaction on 1 μm Ni(ED). However, the $(Cu,Ni)_6Sn_5$ phase was not observed on 3 μm Ni(ED). Interestingly, the Ni_3Sn_4 morphology seems to be different, somewhat finer than the Ni_3Sn_4 grains observed on the electrolytic Ni without the Cu overlayer (refer to Fig. 2(c) and (d). This difference in the IMC morphology may be due to the Cu overlayer.

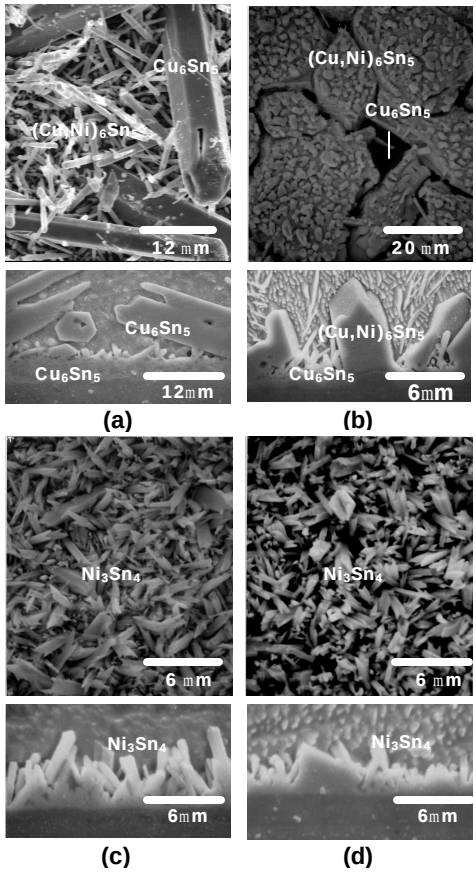

Fig.5. SEM micrographs of IMC morphologies of Cu/Ni(EL)/Sn samples in the top and cross-sectional views after reflow for 10 min at 250°C; on (a) 0.3 mm Ni-P (EL), (b) 0.6 mm Ni-P (EL), (c) 3 mm Ni-P (EL) and (d) 10 mm Ni-P (EL)

In the case of 0.3 μm Cu, the $(Cu,Ni)_6Sn_5$ exists after 2 min, in Fig. 8(a) and (c). After 10 min, however, the $(Ni,Cu)_3Sn_4$ occupies mostly the interface on 3 μm Ni in Fig. 8(b), while $(Cu,Ni)_6Sn_5$ is the dominant phase

on 1 μm Ni, in Fig. 8(d). The IMC phases formed on 1μm and 3 μm Ni(ED) were confirmed by the XRD patterns in Fig. 9(a) and (b). On 1 μm Ni(ED), Cu_6Sn_5 phase is dominant, while on 3 μm, Ni_3Sn_4 phase is the major phase.

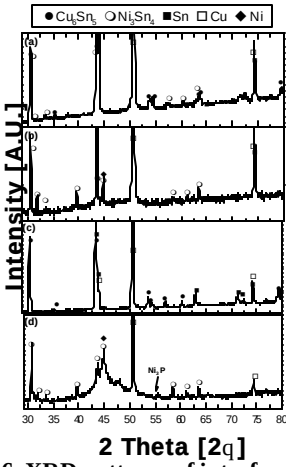

Fig.6. XRD patterns of interfaces of Cu/Ni(EL)/Sn samples reflowed at 250 °C ; on (a) 0.3 μm Ni-P (EL), (b) 0.6 μm Ni-P(EL) after 2 min , (c) 0.3 μm Ni-P(EL) and (d) 10 μm Ni-P(EL) after 10 min

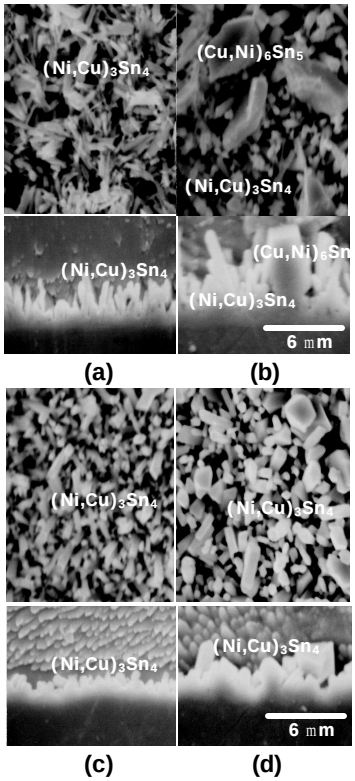

Fig.7. SEM micrographs of IMC morphologies of Cu/Ni(ED)/Cu(ED)/Sn in the top and cross-sectional views reflowed ; (a) after 2 min and (b) 10 min on 1 μm Ni(ED)/0.04 μm Cu(ED) and (c) after 2 min and (d) after 10 min on 3 μm Ni(ED)/0.1 μm Cu(ED).

The IMC morphologies on 0.5 μm Cu are shown in Fig. 10 in the top and cross-sectional views after 2 and 10 min. Because of the thick Cu layer, the reaction product is the $(Cu,Ni)_6Sn_5$ phase even after 10 min. And also, the $(Cu,Ni)_6Sn_5$ phases on 1 μm and 3 μm Ni(ED) appear to have a similar morphology, but different from those on thin Ni(ED) without Cu overlayer (refer to Fig. 1(a), Fig. 2 (a) and (b). This difference in morphology may be attributed to the difference in Ni content of the $(Cu,Ni)_6Sn_5$.

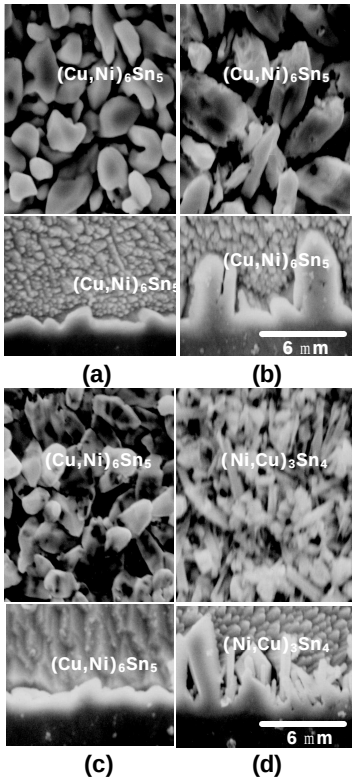

Fig.8. SEM micrographs of IMC morphologies in the top and cross-sectional views reflowed ; (a) after 2 min and (b) 10 min on 1 μm Ni(ED)/0.3 μm Cu(ED) and (c) after 2 min and (d) after 10 min on 3 μm Ni(ED)/0.3 μm Cu(ED).

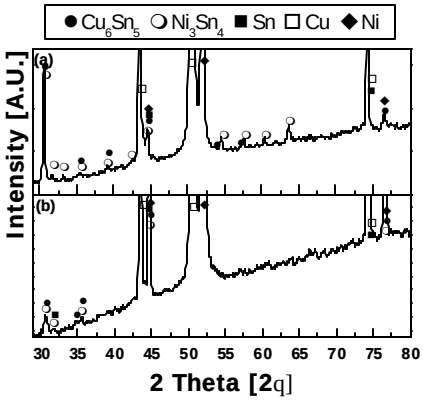

Fig.9. XRD patterns of interfaces of Cu/Ni(ED)/Cu(ED)/Sn samples reflowed at 250 °C for 10 min; on (a) 1 μm Ni(ED) / 0.3 μm Cu(ED) and (b) 3 μm Ni(ED) / 0.3 μm Cu(ED).

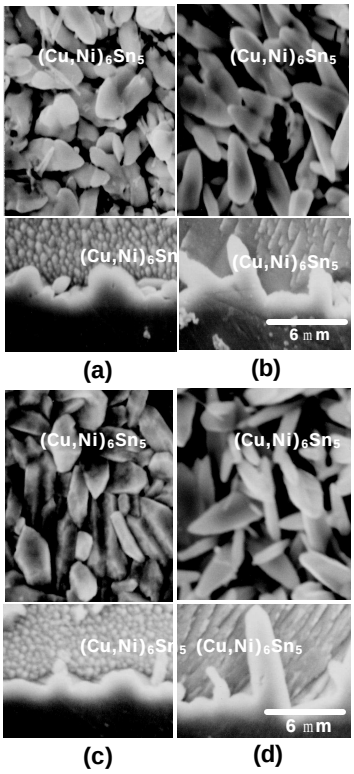

Fig.10. SEM micrographs of IMC morphologies of Cu/Ni(ED)/Cu(ED)/Sn samples in the top and cross-sectional views reflowed ; (a) after 2 min and (b) 10 min on 1 mm Ni(ED)/0.5 mm Cu(ED) and (c) after 2 min and (d) after 10 min on 3 mm Ni(ED)/0.5 mm Cu(ED).

DISCUSSION

In this study, three major variables have been chosen to demonstrate how they affect the interfacial reactions: Ni thickness, Ni plating type, and thickness of the Cu overlayer on Ni. The effects of three variables are discussed in terms of IMC morphology and phase identification.

Effect of Ni Thickness on IMC Phases

Table I summarizes the XRD results of IMC phase identification as a function of Ni thickness and reflow time. The IMC phases are affected by both Ni thickness and reflow time. As the Ni layer gets thinner and the reflow time becomes longer, the formation of the Cu_6Sn_5 phase becomes more favorable than the Ni_3Sn_4 phase. After 2 min, Ni_3Sn_4 is the main IMC phase in all samples and the Cu_6Sn_5 phase is only found on 0.3 μm Ni, while after 10 min, the Cu_6Sn_5 becomes the major phase at the interface on 0.3 μm and 0.6 μm Ni. However, it is interesting to find the type of Ni plating (electrolytic vs electroless) does not influence the IMC phase identification.

Table I Variations of IMC phases in Ci/Ni/Sn samples as a function of Ni thickness and reflow time

Samples	Reflow Time (min).	
Ni(ED) or Ni(EL)	2	10
0.3	$(Cu,Ni)_6Sn_5$>$(Ni,Cu)_3Sn_4$	$(Cu,Ni)_6Sn_5$ > $(Ni,Cu)_3Sn_4$
0.6	$(Ni,Cu)_3Sn_4$	$(Cu,Ni)_6Sn_5$ > $(Ni,Cu)_3Sn_4$
1	$(Ni,Cu)_3Sn_4$	$(Ni,Cu)_3Sn_4$ > $(Cu,Ni)_6Sn_5$
3	Ni_3Sn_4	$(Ni,Cu)_3Sn_4$
10	Ni_3Sn_4	$(Ni,Cu)_3Sn_4$

In general, what kind of IMC would form at the interface can be predicted under the local equilibrium state at the interface [9,10]. Under the local equilibrium, by comparing the activation energies of competing IMCs, the IMC phase that forms first is determined as the one with the smallest activation energy. The value of the activation energy for the formation of Sn-Ni IMC phases between Sn and Ni at 250°C was calculated [10]. The Ni_3Sn_4 phase was found to have the lowest energy, so forming first. And then, the Ni_3Sn_2 and the Ni_3Sn are expected to form after the Ni_3Sn_4 phase. In the present study, as shown in table I, the Ni_3Sn_4 phase is detected in all samples after 2 min, indicating that the Ni_3Sn_4 phase is the first IMC formed in the joints between Sn and Ni layer regardless of Ni thickness. This result agrees well with the previous thermodynamic calculation [10] and the experimental observation between liquid Sn and thick solid Ni [11]. However, the approach using the minimum activation energy cannot apply to the samples reflowed for 10 min, since the calculation is acceptable only at the early stage of the reflow when the sources of the liquid and solid are infinite. In this study, because of the lack of Ni supply to keep the local equilibrium state, the second IMC, Cu-Sn type, forms through the participation of Cu atoms from the Cu underlayer. Therefore, it has changed the local equilibrium state from the Sn-Ni binary system to the Sn-Ni-Cu ternary. And this transition depends on Ni thickness as well as reflow time.

Fig. 11 shows the schematic diagram summarizing the effect of Ni thickness on the IMC phases after 10 min in this study. The Ni_3Sn_4 phase forms first as soon as the reaction gets started, since the Ni_3Sn_4 phase has the lowest activation energy. As the reflow continues, the interfacial reactions become complicated due to the reaction between the Cu underlayer and the molten Sn. When Ni is thinner than 1 μm, Fig. 11(a), Cu atoms easily diffuse through the Ni layer. At the same time, this Ni layer keeps dissolving into the molten Sn, and subsequently the Cu underlayer is exposed to the molten Sn. At that point, the preferential formation and fast growth of the Cu-Sn type

IMC occurs to produce several phases at the interface, such as $(Cu,Ni)_6Sn_5$, Cu_5Sn_6 and Ni_3Sn_4. On the other hand, when Ni is thicker than 1 μm, Fig. 11(b), it may take a much longer time for Cu to diffuse through the Ni layer. Hence the Ni_3Sn_4 phase forms first and continues to grow. This situation would make Cu out-diffusion further suppressed. Due to these reasons, different types of IMCs form depending on the Ni thickness and can affect the reliability of solder joint differently. Therefore, Ni thickness should be considered as an important factor when a Ni layer is applied for a diffusion/reaction barrier to control the interfacial reaction.

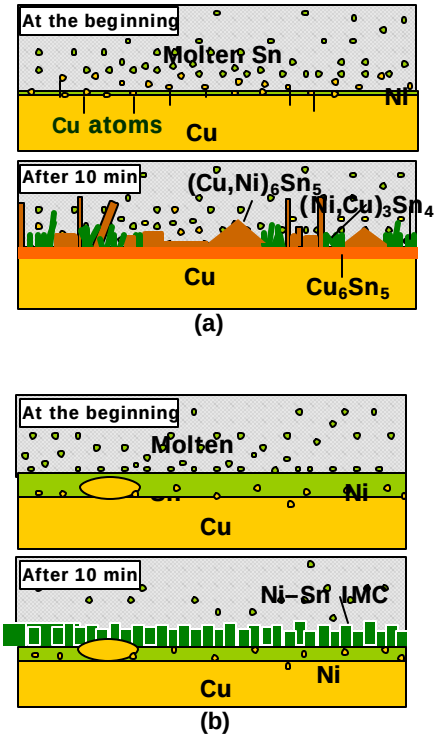

Fig.11. Schematic diagrams showing the effect of Ni thickness on the IMC phases at the beginning and after 10 min ; (a) when Ni < 1㎜ and (b) when Ni > 1㎜

Effect of Ni Plating on Ni_3Sn_4 Morphology

A compact structure of faceted Ni_3Sn_4 grains is observed on the electrolytic Ni(ED), while a porous structure of needle-like Ni_3Sn_4 grains is shown on the electroless Ni(P), Fig.12(b). Ni(ED) is known to have a crystalline structure with a density, 8.1g/cm^3 [12] and forms a similar Ni_3Sn_4 morphology to that of a bulk Ni foil [2]. But Ni-P(EL) is strongly affected by the condition of Ni plating solution, especially P content. With different P content, the structure of Ni(P) layer varies from amorphous, nanocrystalline, crystalline and their mixture [13]. The Ni-P(EL) layers used in this study contain about 16 at% of P, and are expected to be in an amorphous state in the as-plated condition [14]. In addition, the density of Ni-P(EL), about 7.9 g/cm^3, is somewhat smaller than the electrolytic Ni. When a Ni-P(EL) is in contact with a molten Sn, several reactions are possible to occur; dissolution of Ni and P into Sn, Ni_3Sn_4 formation, crystallization of Ni_3P, and others. The presence of P changes the interface composition and thereby makes a difference in the interfacial energies which can influence the IMC morphology as well as IMC nucleation mechanism. The previous work [15] demonstrated that the interfacial energy between molten solder and growing IMC determines whether the IMC has a round or faceted interface. It is also shown that the higher interfacial energy results in the faceted interfaces due to a preferred growth in the plane with the lowest energy. Thus the narrow needle-like Ni_3Sn_4 grains observed on Ni-P(EL) can be attributed to the higher interfacial energy due to the existence of P at the interface, in comparison with the faceted and angular grains on Ni(ED). In addition, the porous structure observed on the electroless Ni(P) can be understood in terms of the formation of Ni_3P. Since the Ni_3P layer forms between the Ni-Sn IMC and Ni-P(EL), it would cause poor adhesion of Ni_3Sn_4 to the interface and alter the nucleation mechanism of IMC at the interface. In fact, some evidence of poor adhesion or spalling of Ni-Sn IMC and different IMC morphologies on Ni(P) were reported in various Pb-free solder joints [2,16]. In this study, the IMC morphology on Ni-P did not exhibit such poor adhesion or spalling from the interface, but a thick porous structure of Ni_3Sn_4 IMCs is observed.

Effect of Cu Thickness over Ni on IMC phases

Table II summarizes the change in IMC phases as a function of Cu thickness and reflow time on 1 and 3 μm Ni. For 2 min reflow, the change in IMC phases as a function of Cu thickness shows the same trend for 1 μm and 3 μm Ni. It is clear that the IMC phases depend strongly on Cu thickness. The dominant IMC phase varies from Ni_3Sn_4 to η-Cu_6Sn_5 as Cu becomes thicker. For 10 min reflow, it is found that both Cu and Ni thickness become important in determining the intermetallic phases. This can be understood by noting that Cu atoms to form the Cu-Sn (or Cu-Ni-Sn) IMCs can be supplied from both the Cu over- and underlayer depending on the Ni thickness. It is also found that 2 min reflow is not long enough to melt 0.3 μm Cu completely, by detecting the $(Cu,Ni)_6Sn_5$ phase and the residual Cu layer at the interface, although the entire dissolution of 0.3μm Cu would not satisfy the solubility limit of Cu into 40 μm molten Sn at 250°C. After 10 min reflow, the interface becomes complicated with two mixed IMC phases, $(Cu,Ni)_6Sn_5$ and Ni_3Sn_4.

In case of 1 μm Ni, η-Cu_6Sn_5 forms dominantly for the thick Cu, 0.3 μm and 0.5 μm,

suggesting the contribution of the Cu underlayer. In these cases, during the reflow, the Cu layer dissolves, and simultaneously Cu atoms from the underlayer diffuse through the Ni layer and come to contact with the molten Sn. That is, the loss of Cu due to the melting is compensated with the Cu from the underlayer. Therefore, the $(Cu,Ni)_6Sn_5$ phase can continue to grow and occupy most of the interface. In the case of 3 μm Ni, the Cu underlayer would not affect the interfacial reactions. Thus only the thickness of Cu overlayer would determine the interfacial reaction. For 3 μm Ni with 10 min reflow, Ni_3Sn_4 IMC is dominant for 0.1 and 0.3 μm Cu, while for 0.5 μm Cu, $(Cu,Ni)_6Sn_5$ forms as a continuous layer with Ni_3Sn_4 IMC grown underneath the $(Cu,Ni)_6Sn_5$..

Table II. Variations of IMC phases in Cu/Ni/Sn samples as a function of Cu thickness and reflow time on 1 μm Ni and 3 μm Ni

Samples			Reflow Time (min)	
Ni (μm)	Cu (μm)	(wt%)	2	10
1	0.04	0.1	$(Ni,Cu)_3Sn_4$ > $(Cu,Ni)_6Sn_5$	$(Cu,Ni)_6Sn_5$ ~ $(Ni,Cu)_3Sn_4$
	0.3	0.8	$(Cu,Ni)_6Sn_5$	$(Cu,Ni)_6Sn_5$ > $(Ni,Cu)_3Sn_4$
	0.5	1.4	$(Cu,Ni)_6Sn_5$	$(Cu,Ni)_6Sn_5$
3	0.1	0.3	$(Ni,Cu)_3Sn_4$ > $(Cu,Ni)_6Sn_5$	$(Ni,Cu)_3Sn_4$ > $(Cu,Ni)_6Sn$
	0.3	0.8	$(Cu,Ni)_6Sn_5$	$(Ni,Cu)_3Sn_4$ > $(Cu,Ni)_6Sn$
	0.5	1.4	$(Cu,Ni)_6Sn_5$	$(Cu,Ni)_6Sn_5$ > $(Ni,Cu)_3Sn_4$

In Table II, the Cu composition in Sn-Cu alloys has been estimated for each Cu thickness by assuming the entire Cu overlayer to dissolve into 40 μm Sn. However, as shown in Table II, the major IMC phase can be different depending on Ni thickness. For example, in the case of 10 min reflow, Cu-Sn IMC is the major phase for 1 μm Ni, while Ni-Sn is the major phase for 3 μm Ni.

CONCLUSION

From this study, the following conclusions have been drawn.

1. IMC morphology is strongly affected by the type of Ni plating, electrolytic vs. electroless. The angular or faceted Ni_3Sn_4 is observed on electrolytic Ni, while needle-like IMC on electroless Ni(P). The presence of Cu changes the interfacial microstructure significantly by forming the ternary IMC, $(Cu.Ni)_6Sn_5$ phase, which grows more aggressively than the binary Cu-Sn or Ni-Sn IMCs..

2. The IMC phases in Cu/Ni/Sn joints are determined by Ni thickness and reflow time due to the involvement of Cu underlayer. Ni_3Sn_4 is detected in all samples for short reflow, indicating that Ni_3Sn_4 is the first-forming IMC phase on Ni layer. For long reflow time, when Ni is less than 1 μm thick, Cu underlayer affects the interfacial reactions significantly, resulting in the fast growth of $(Cu,Ni)_6Sn_5$.

3. The Cu overlayer in Cu/Ni/Cu/Sn joints affects IMC phases depending upon both Ni and Cu thickness. For thin Cu, $(Ni,Cu)_3Sn_4$ forms dominantly, while for thick Cu, $(Cu,Ni)_6Sn_5$ is the major phase.

4. The present study can help to better understand the interfacial reactions of Pb-free solders and thereby impact on improving their reliability performance of Pb-free solder joints.

REFERENCES

1. R. Tummala, Fundamentals of Microsystems Packaging (McGraw Hill, New York, 2000), Chap. 9.
2. S. K. Kang, Proc. 51st Elec. Comp. Tech. Conf., Proc. 51st Elec. Comp. Tech. Conf. Orlando, FL., p.448-454 (2001).
3. W. K. Choi, S. K. Knag and D.-Y. Shih, to be published in in JEM, November (2002).
4. J. W. Jang, D. R. Frear, T. Y. Lee and K. N. Tu, J. Appl. Phys., Vol. 88, pp.6359-6363 (2000).
5. A. Zribi, A. Clark, L. Zavalij, P. Borgesen, and E. Cotts, J. Electronic Materials, Vol.30(9), pp.1157-1164, (2001)
6. K. Zeng, V. Vuorinen and J. Kivilahti, Proc. 51st Elec. Comp. Tech. Conf. Orlando, FL. pp.693-698, (2001).
7. W. T. Chen, C. E. Ho and C. R. Kao, J. Mater. Res., Vol. 17, pp. 263-266 (2002).
8. C. E. Ho, R. Y. Tsai, Y. L. Lin and C. R. Kao, J. Elec. Mater., Col. 31, pp. 584-590 (2002).
9. B.-J. Lee, N.-M. Hwang and H. M. Lee, Acta Mater., vol. 45, pp. 1867-1874 (1997).
10. W. K. Choi and H. M. Lee, Scripta Mater., no. 11, pp. 777-781 (2002).
11. S. K. Kang and Ramachandran, Scripta Metall., Vol.14 (4), pp.421-424, (1980).
12. William H. Safranek, "The Properties of Electrodeposited Metals and Alloys" A Handbook, Elsevier, pp.219-289, (1974).
13. B. Färber, E. Cadel, A. Menand and G. Schmitz, Acta. Mater., vol. 48, pp. 789-796 (2000).
14. Y. C. Sohn, J. Yu, S. K. Kang, W. K. Choi and D.-Y. Shih, to be published in J. Mater. Res. January, (2003).
15. W. K. Choi, S.-Y. Jang, J. H. Kim, K.-W. Paik and H. M. Lee, J. Mater. Res., vol. 17, pp. 597-599 (2002).
16. J. W. Jang, P. G. Kim, K. N. Tu , D. R. Frear and P. Thompson, J. Appl. Phys., vol. 85, pp. 8456-8463 (1999).